Journal of Optoelectronics and Advanced Materials Vol. 7, No. 4, August 2005, p. 2021 - 2027

ELECTRICAL AND OPTICAL PROPERTIES OF Sb_xS_{1-x} ALLOYS

T. Shchurova*, N. Savchenko, V. M. Rubish[a], V. V. Rubish, A. Spesivykh, I. Opachko

Uzhgorod National University, Department of Engineering, 13 Kapitulna St., 88000 Uzhgorod, Ukraine
[a]Uzhgorod Scientific-Technological Center of the NASU Institute for Information Recording, 4 Zamkovi Skhody Str., Uzhgorod 88000, Ukraine

The valence-band maximum, the conduction-band minimum,, the position of the electronic states in quasi band gap formed by homopolar Sb-Sb bonds and clusters S_n for chalcogenide glassy alloys of Sb_xS_{1-x} ($0.35 \le x \le 0.45$) family have been calculated on the basis of the method suggested by W.A. Harrison. Spectral dependences of the photoelectron quantum yield, absorption coefficient, photoluminescence and photoconduction for $Sb_{0.40}S_{0.60}$ have been presented. The photoemission threshold, the optical band gap, and the energies of the radiative and band-to-band transitions have been determined from these dependences, respectively. The experimental and calculated energy parameters have been correlated. Experimental and calculated concentration dependences of the optical band gap, thermal activation energy and energy position of the peak in photoconduction spectra for $Sb_{0.35}S_{0.65}$, $Sb_{0.38}S_{0.62}$, $Sb_{0.40}S_{0.60}$, $Sb_{0.43}S_{0.57}$, and $Sb_{0.45}S_{0.55}$, have been given.

(Received May 24, 2005; accepted July 21, 2005)

Keywords: Chalcogenide semiconductors, Electronic structure, Optical properties

1. Introduction

The results of the earlier studies of Sb_xS_{1-x} (x = 0.35 - 0.45) glassy alloys have shown that short-range parameters undergo non-monotonic changes with concentration of antimony [1]. For these materials the peculiarities in density, softening point, d. c. conduction activation energy, and photon energy position of the peak in photoconduction behaviour have been observed in the concentration dependences above and below x = 0.40 [2]. Raman spectra studies have revealed that for glassy alloys of the compositions with x = 0.36, 0.40, 0.43, the band at 200 cm^{-1} is attributed to the presence of the ring-shaped S_8 molecules in the matrix, when the band at 155 cm^{-1} for x in the range from 0.36 to 0.70 can be related to the vibrations of the homopolar Sb–Sb bonds realized in $SbSb_{3/3}$ structural units [3].

For the simulation of the energy bands and electronic states in the band gap of crystalline semiconductors the method based on the linear combination of the atomic orbitals and pseudopotential is developed [4]. As far as the radius of the first coordination sphere in amorphous phase (0.250 nm [5]) is close to the average distance between the neighbouring atoms in Sb_2S_3 crystals (0.251 nm) it should be expected, that the band structure is determined, mainly, by the overlapping integral between the neighbouring atoms. Moreover, the local atomic arrangement in amorphous phase is not too much different from that in the crystal. Thus we have used the mentioned method for the calculation of the energy bands and electronic states formed by clusters S_n and homopolar Sb–Sb bonds in quasi band gap.

Experimental results on photoemission, absorption edge, photoluminescence and photoconduction for SbS_3 glasses and correlation of them with the respective data for As_2S_3 glasses give important information. This work is devoted to the correlation of experimental and calculated

* Corresponding author: taina@tv.uzhgorod.ua

concentration dependences of optical band gap, thermal activation energy and energy position of the peak in photoconduction spectra for Sb_xS_{1-x} alloys.

2. Experimental

Glasses of Sb_xS_{1-x} (x = 0.35÷0.45) family have been prepared by the slow melting of the mixtures of high purity Sb and S (99.999 %) in silica ampoules evacuated to 10^2 Pa with a subsequent rapid quenching of the melt at the rates from 100 to 300 K/s. Glass densities have been measured by the densimeter with a relative error less than 0.1 %.

Photoemission quantum efficiency spectra have been obtained with the help of monochromator with linear dispersion of 1.6 nm/mm. Registration system operated in pulse counting mode with background signal subtraction, photocurrent sensitivity being in the range of $(1\text{-}3)\times10^{-19}$ A. The photoemission threshold energy has been determined with an accuracy of 0.1 eV. For the optical band gap of the glass the energy of photons corresponding to the absorption coefficient of 10^3 cm^{-1} has been taken.

The energy parameters have been determined following the conventional procedure from photoluminescence spectra. The photoluminescence spectra have been measured at 77 K, the other measurements have been performed at room temperature.

3. Computational procedure

The calculation of the energy band structure for Sb_xS_{1-x} alloys under investigation has been performed by the linear combination of atomic orbitals (LCAO) method [4] in the following steps:

1. The magnitudes of the energies corresponding to the valence-band maximum E_v), the conduction-band minimum (E_c) have been calculated for the consistent elements (Sb and S) and binary compound (Sb_2S_3) following the equations:

$$E_v^{Sb\text{-}S} = (\varepsilon_p^{Sb} + \varepsilon_p^{S})/2 - (V_2^2 + V_3^2)^{1/2} - \Delta E_{s\text{-}o} + V_1^{\sigma} + U/2, \quad (1)$$

$$E_c^{Sb\text{-}S} = (\varepsilon_p^{Sb} + \varepsilon_p^{S})/2 + (V_2^2 + V_3^2)^{1/2} - V_1^{\sigma^*} + U/2, \quad (2)$$

where all the parameters, except matrix element V_2 characterizing the covalent bond ionicity, can be found from the atomic terms calculated within Hartree Fock approximation: ε_p^S = -11.60 eV and ε_p^{Sb} = -11.60 eV [6]. The value $V_2 = \eta_1 \times h/2\pi m d_1^2$, $\eta_1 = (\eta_{pp\sigma}^2 + \eta_{pp\pi}^2)^{1/2} = 2.39$ has been determined following [7], where η_1 - coefficient which determines the value of the interatomic interaction matrix element, d_1 - is an average distance between Sb and S atoms (experimental values for the radii of the first coordination sphere have been used [1]). The matrix element V_3 standing for polar bond energy has been calculated as $V_3 = (\varepsilon_p^{Sb} - \varepsilon_p^{S})/2 = 1.73$ eV. The values for intratomic Coulomb repulsion U have been derived from [6] as $U = x \times U^{Sb} + (1\text{-}x) \times U^{S}$, where U^S = 9.44 eV and U^{Sb} = 7.92 eV. The metallic bond energy over bonding (V_1^{σ}) and antibonding ($V_1^{\sigma^*}$) states has been calculated with account of the correction for the polarity a_p [6].

Spin-orbital splitting of the valence band for Sb_xS_{1-x} has been derived as

$$\Delta E_{s\text{-}o} = (1 + a_p)\,\Delta E_{s\text{-}o}^{S}/2 + (1 - a_p)\,\Delta E_{s\text{-}o}^{Sb}/2, \qquad a_p = V_3 / (V_2^2 + V_3^2)^{1/2}. \quad (3)$$

where $\Delta E_{s\text{-}o}^{S}$ and $\Delta E_{s\text{-}o}^{Sb}$ values have been taken as 0.074 eV and 0.973 eV, respectively from [8].

The splitting of LP-states for Sb_xS_{1-x} has been calculated from $\Delta E_{LP} = \eta_{pp\sigma} \times h/2\pi m d_2^2$, where $\eta_{pp\sigma}$ = 0.50 [4], d_2 = 0.207 nm [9] - interatomic distance between sulphur atoms. The top of LP band has been found to be of about -5.99 eV for ΔE_{LP} = 0.89 eV from the equation:

$$E'_{LP} = \varepsilon_p^S + \Delta E_{LP} + U^S/2; \quad (4)$$

2. The energy positions of the electronic states formed by the homopolar Sb-Sb bonds, E_1, and by the clusters composed of the identical sulphur atoms, E_2, have been found from the equations:

$$E_1 = \varepsilon_p^{Sb} + \eta_1 \times h/2\pi m d_3^2, \qquad E'_1 = \varepsilon_p^{Sb} + \eta_2 \times h/2\pi m d_3^2, \quad (5)$$

$$E_2 = \varepsilon_p^S + \eta_1 \times h/2\pi m d_4^2 + U/2, \quad E'_2 = \varepsilon_p^S + \eta_3 \times h/2\pi m d_2^2 + U/2, \quad (6)$$

where $\eta_2 = (\eta_{sp\sigma}^2 + \eta_{pp\sigma}^2)^{1/2} = 2.64$, $\eta_3 = \eta_{ss\sigma} = 1.32$, d_3 is Sb-Sb interatomic distance taken as 0.280 nm , d_4 is the shortest distance between sulphur atoms in different layers taken as 0.263 nm.

The energy position of the Fermi level has been calculated as $E_F = (E_v - E_c)/2$ for x = 0.35 - 0.43 and $E_F = (E'_2 - E'_1)/2$ for x = 0.45.

3. The energy band diagrams have been constructed from the data obtained above, and the optical band gap E_o, thermal activation energy E_a, the energy position of the peak in photoluminescence E_{phlum}, the energy position of the peak in photoconduction spectra E_{ph}^{max} have been determined for the alloys of different compositions.

4. Results

The Table presents the average values of the interatomic distances for Sb_xS_{1-x} (x = 0.35 - 0.45) alloys, matrix elements for the covalent bond energy, the energy of splitting into bonding and antibonding orbitals ($(V_2^2 + V_3^2)^{1/2}$), metallic bond energy over bonding and antibonding orbitals, bond polarity, spin-orbital splitting, splitting energy for S *3p* LP-states, Coulomb intratomic repulsion energy, the valence-band maximum determined from the position of the bonding Sb *5p* - S *3p* orbitals, the conduction-band minimum determined from the position of the antibonding Sb *5p* - S *3p* orbitals, the Fermi level and levels formed by S_n (E_2) and S'_n (E'_2) clusters.

Table. The interatomic distances, matrix elements and predicted band energy values for Sb_xS_{1-x} alloys.

Parameters	x = 0.35	x = 0.38	x = 0.40	x = 0.43	x = 0.45
d_1, nm	0.255	0.260	0.250	0.260	0.265
V_2, eV	2.80	2.69	2.91	2.69	2.59
$(V_2^2 + V_3^2)^{1/2}$, eV	3.29	3.20	3.39	3.20	3.11
V_1^{σ}, eV	2.84	2.85	2.84	2.85	2.85
$V_1^{\sigma^*}$, eV	2.24	2.23	2.24	2.23	2.23
α_p	0.53	0.54	0.51	0.54	0.55
$\Delta E_{s\text{-}o}$, eV	0.28	0.29	0.28	0.29	0.28
U/2, eV	4.45	4.43	4.42	4.39	4.38
$-E_v$, eV	6.16	6.08	6.30	6.12	6.03
$-E_c$, eV	4.37	4.47	4.31	4.51	4.61
$-E_F$, eV	5.27	5.28	5.15	5.17	5.22
E_2, eV	4.52	4.54	4.55	4.58	4.61
E'_2, eV	4.80	4.82	4.83	4.86	4.87

Fig. 1 shows the changes in E_c, E_v, E_F, E_2, and E'_2 values with the content of antimony atoms for Sb_xS_{1-x} alloys. Here we see also the position of the energy levels formed by the homopolar Sb-Sb bonds $E_1 = -5.82$ eV and $E'_1 = -5.57$ eV, as well as the position of the top of LP band $E'_{LP} = -5.99$ eV for Sb_xS_{1-x} glasses. Arrows show the transitions between the energy levels that fit the best experimental results: optical (solid), radiative (dotted) transitions and thermal activation energy (dashed).

Fig. 2 shows the spectral dependences of: a) photoemission quantum yield; b) absorption coefficient near the fundamental absorption edge (curve 1) and photoconduction (curve 2); c) photoluminescence for Sb_2S_3 glasses. The data for As_2S_3 glasses are given for the comparison. The absorption edge and photoconduction for As_2S_3 glasses have been taken from reference [10], the data for Sb_2S_3 glasses - from [2]. Extrapolation of the steep parts of $Y^{1/3} \div E$ dependences to zero value (Fig. 2, a) give equal energy values of 6.2 eV for both compounds. Extrapolation of the flat parts of these dependences to zero value give the energy values for As_2S_3 and Sb_2S_3 glasses of 5.0 eV and 5.5 eV, respectively. The emission of photoelectrons for Sb_2S_3 glasses was terminated at 5.9 eV. The calculated values for these parameters have been found to be 6.30 eV and 5.96 eV, respectively. From Fig. 2, b, we can see that in contrast to As_2S_3 glasses, the photon energy related to the maximum in photoconduction spectra for Sb_2S_3 glasses is shifted towards the weak absoption tail. Emission spectrum for Sb_2S_3 glasses shows two peaks in intensity at 0.75 eV and 1.0 eV (Fig. 2, c). The about calculated values for the position of the peaks in radiative transitions have been calculated to be 0.77 eV and 0.99 eV.

Fig. 3 presents experimental and calculated concentration dependences of: a) optical band gap; b) thermal activation energy; c) photon energy position of the photoconduction peak for glassy Sb_2S_3. From this figure it is seen that theory and experiment are in good agreement.

It is remarkable that in Ref. [12] the optical gap due to direct transitions, in annealed amorphous films of Sb_2S_3 is 2.40 eV while for indirect transitions is 1.64 eV.

5. Discussion

As it is seen from the Table, the highest change in $2 \times (V_2^2 + V_3^2)^{1/2}$ value that is usually responsible for the optical band gap in semiconductors has been found to be of about 0.56 eV for glassy Sb_xS_{1-x}, when the experimentally observed one is about 0.1 eV. The coincidence in the photoemission thresholds (6.2 eV) for Sb_2S_3 and As_2S_3 glasses (Fig. 2, a) testifies that the valence-band maximum in these materials is formed by the lone pair *p*-electron states (S *3p*) of sulphur atoms. The peak in photoconduction for Sb_2S_3 is observed at photon energy lower than the optical band gap, being in favourof the existence of the electron states below the conduction-band minimum (Fig. 2, b, curve 1). The results of the calculations that are given in Fig. 1 show the possible optical transitions. The experimentally determined optical band gap at $\alpha = 10^3$ cm^{-1} for Sb_xS_{1-x}, alloys corresponds to all possible optical transitions observed in chalcogenide semiconductors. Thus, for $Sb_{0.40}S_{10.60}$ and $Sb_{0.35}S_{10.65}$ these are the transitions from the localized (E'_{LP}) to the nonlocalized (E_c) states and vice a versa ($E_v \rightarrow E_2$), when for the other compositions they are band-to-band transitions. The band-to-band transitions are determined by the position of the mobility threshold in the valence band formed by the by the bonding Sb *5p* - S *3p* orbitals (E_v), and the one in the conduction band, formed by antibonding Sb *5p* - S *3p* orbitals (E_c).

From Fig. 2, a, b, c it follows, that in Sb_2S_3 above the valence band formed by LP states (E'_{LP}) the electronic states extending into the band gap and giving rise to the tail in photoemission and weak absorption tail take place. Their existence results in the photoconduction in this spectral range (Fig. 2, b, curve 1). The photoluminescence spectra given in Fig. 2, c indicate the presence of two deep evels of radiative recombination in Sb_2S_3.

Equations 5 and 6 for E_1, E'_1, E_2, and E'_2 specify the atomic orbitals taking part in the formation of the electronic states in the band gap. The electronic states E_1 formed by Sb-Sb wrong bonds are located near the valence band (E'_{LP}). This arrangement of the levels fits the energy band model without charged defects suggested by Tanaka (see, model *a* [10]). It may be assumed that under the excitation by light and at the excess of Sb ($x \geq 0.45$) the *sp* hybridization of Sb-Sb bonds

takes place, resulting in the conversion of the part of $pp\pi$ orbitals into the $sp\sigma$ ones. This gives rise to the electronic states E'_1 in the band gap.

The electronic states E_2 below the conduction-band minimum are formed by the clusters of sulphur atoms S_n (Fig. 1). They could be the S_8 rings or S_n chains. Deeper are the electronic states E'_2 arising in result of the absorption of photon. One of the qualitative models for the photostructural changes is described in [11]. According to it, under the excitation of the electrons by the light the van der-Waals interaction between S'_n atoms in the neighbouring chains ($d \sim 0.33$ nm) is changed for the stronger Coulomb interaction. Our calculations have shown that before illumination electronic states of S'_n atoms are found at the energy of ~ -6.3 eV. Under the photon absorption the S atoms is turned towards the closest S atom resulting in the interatomic distance equal to 0.207 nm, and electronic S'_n states fall within the band gap (E'_2).

The energy diagrams given in Fig. 1 allows the explanation of the photoluminescence spectra for Sb_2S_3 (Fig. 2, c) and the concentration dependences of E_o, E_a and E_{ph} (Fig. 3, c).

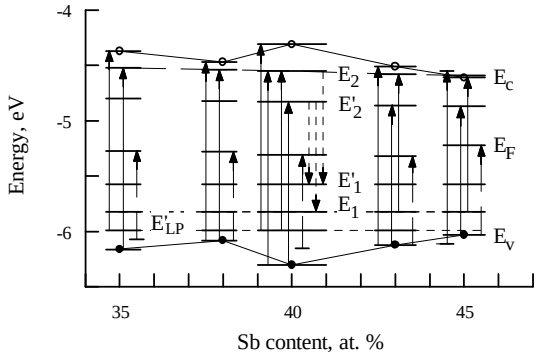

Fig. 1. Sb content dependence of the conduction-band minimum (E_c), the valence-band maximum (E_v), the Sb-Sb homopolar bond energy (E_1, E'_1), S_n (E_2) and S'_n (E'_2) cluster levels, the Fermi level (E_F). E'_{LP} is the position of the top of LP band for Sb_xS_{1-x} glasses. Arrows show optical (solid) and radiative (dotted) transitions, and thermal activation energy (dashed).

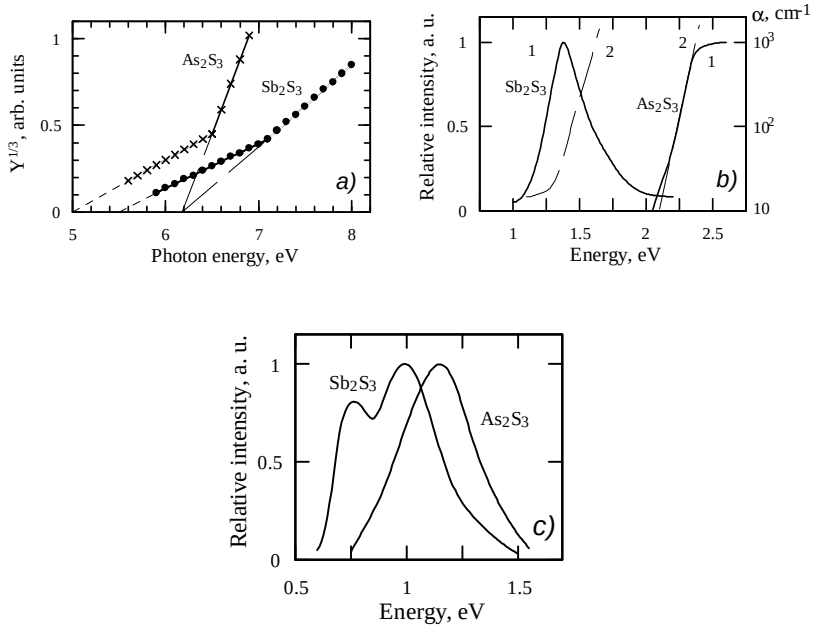

Fig. 2. Photoemission quantum yield versus photon energy for Sb_2S_3 (1) and As_2S_3 (2) glasses (a); photoconduction spectrum (curve 1) and fundamental absorption edge (curve 2) (b); and photoluminescence spectra for glassy Sb_2S_3 and As_2S_3 (c).

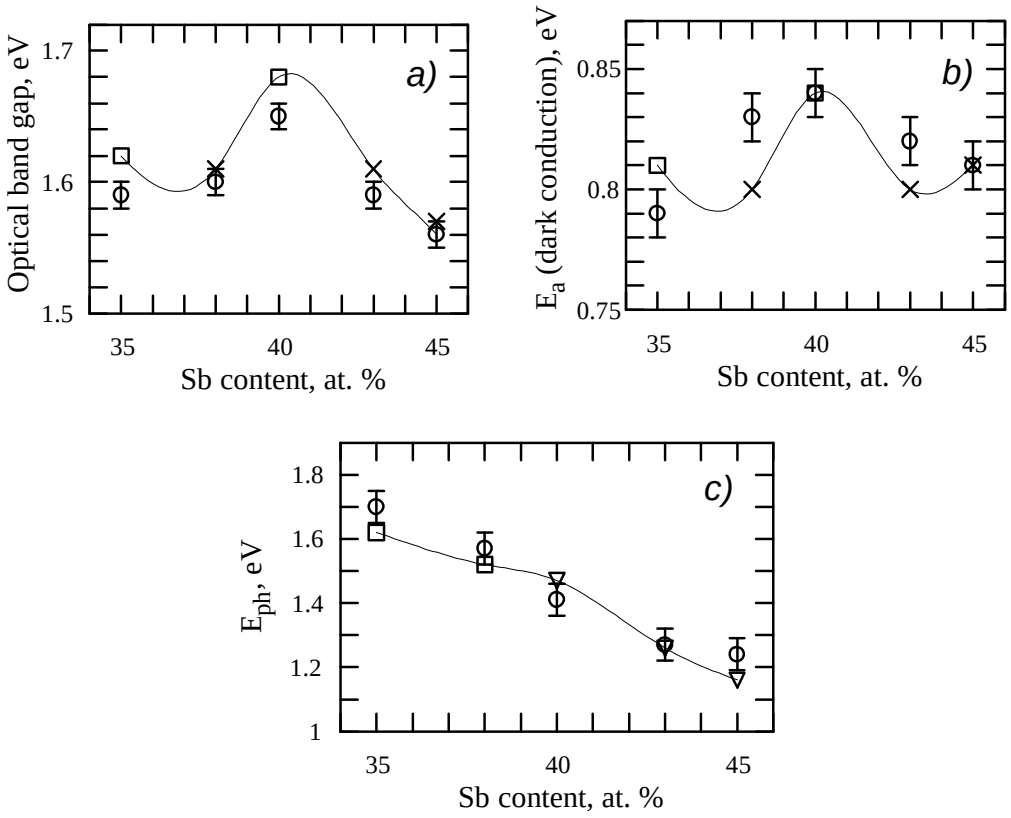

Fig. 3. Experimental and calculated Sb content dependence of the optical band gap (a), thermal conduction activation energy (b), the energy related to the peak in photoconduction spectra (c) for Sb_xS_{1-x} glasses. Circles show experimental data. Squares correspond to $E_v \rightarrow E_c$, or $E_v \rightarrow E_F$ transitions, crosses - to $E_{LP} \rightarrow E_c$ or $E_{LP} \rightarrow E_F$ and triangles -to $E_v \rightarrow E'_2$. Lines present interpolated theoretical data and are given as a guide to the eye.

5. Conclusions

The computation procedure for electronic structure of Sb_xS_{1-x} glasses has been suggested. The quantitative agreement of the computed optical band gap nd photoemission threshold with the experimental results has been found. The valence-band maximum for Sb_2S_3 is formed by the lone pair *p*-electron states of sulphur atoms. The conduction-band minimum is formed by the anti-bonding state of Sb-S bonds. Electronic states of homopolar Sb-Sb bonds are localized above the valence band, when the states of Sb_n clusters are localized below the conduction band. The energy band diagram allows explanation of concentration dependences for the optical band gap, thermal activation energy and energy position of the peak in photoconduction spectra, and peculiarities in photoluminescence and photoconduction spectra.

References

[1] P. P. Shtez, V. M. Rubish, V. L. Malesh, O. G. Guranich, Extended Abstr. XIIIth Inter. Symposium on Non-oxide Glasses and New Optical Glasses, Part I, Pardubice (Czech Republic) 2002. P. 137.

[2] P. P. Shtez, D. I. Bletskan, I. D. Turianitsa, M. P. Bodnar, V. M. Rubish, Proc. Acad. Sci. USSR. Inorg. Materials, **25** (6) 933 (1989).
[3] V. M. Rubish, A. A Stephanovich, P. P. Shtez, V. S. Gerasimenko, I. D. Turianitsa,. V. Yu. Slivka, J. Appl. Spectroscopy, **52** (1), 53 (1990).
[4] W. A. Harrison, Elementary Electronic Structure. World Scientific Publishing Co., New Jersey, London, Singapore, Shanghai, Hong Kong, Taipei, Chennai (2004); W. A. Harrison, Elementary Electronic Structure, World Scientific Publ. Co, Singapore (1999); W. A. Harrison, Electronic Structure and the Properties of Solids. The Physics of the Chemical Bond, W. H. Freeman & Company, San Francisco (1980).
[5] V. P. Zaharov, V. S. Gerasimenko, Structural Peculiarity of the Semiconductors in Amorphous State, Naukova dumka (Scientific Thought) Publ. Co, Kiev (1976).
[6] W. A. Harrison, Phys.Rev. **B 31**, 2121 (1985).
[7] W. A. Harrison, Phys.Rev. **B 41**, 6008 (1990).
[8] D. J. Chadi, Phys. Rev., **B 16**, 790 (1977).
[9] K. K. Shwartz, Physics of Optical Recording in Insulators and Semiconductors, Zinatne, Riga (1986).
[10] Ke. Tanaka, J. of Optoelectronics and Advanced Materials, **3** (2), 189 (2001).
[11] Ke. Tanaka, J. Non-Cryst. Sol. **59/60**, 925 (1985).
[12] N. Tigau, V. Ciupina, G. Prodan, G. I. Rusu, C. Gheorghies, E. Vasile J. Optoelectron. Adv. Mater. **6**(1), 211 (2004).